Fizyka Nyzkykh Temperatur/Low Temperature Physics, 2024, Vol. 50, No. 6, pp. 494–499

Low-temperature magnetic interactions in the "butterfly"-type $\{Fe_3GdO_2\}$ compound: The persistence of magnetic chains

J. Rubín[1,2], A. Arauzo[1,3], F. Bartolomé[1,3], D. Prodius[4,5], and J. Bartolomé[1,3]

[1]*Instituto de Nanociencia y Materiales de Aragón (INMA), CSIC, Universidad de Zaragoza, Zaragoza 50009, Spain*

[2]*Dept. Ciencia y Tecnología de Materiales y Fluidos, Universidad de Zaragoza, Zaragoza 50018, Spain*

[3]*Dept. Física de la Materia Condensada, Universidad de Zaragoza, Zaragoza 50009, Spain*

[4]*Institute of Chemistry, Academy of Science of Moldova, Chisinau MD-2028, Republic of Moldova*

[5]*Critical Materials Innovation Hub, Ames National Laboratory, U. S. Department of Energy, Ames, Iowa 50011, USA*

E-mail: jrubin@unizar.es

Received February 6, 2024, published online April 26, 2024

Heat capacity measurements on the Ln = Gd case of the butterfly molecule series $[Fe_3Ln(\mu_3\text{–}O)_2(CCl_3COO)_8(H_2O)(THF)_3]$, in brief $\{Fe_3LnO_2\}$, is presented. In the previously studied $\{Fe_3YO_2\}$ butterfly, where the magnetic properties stem only from the Fe^{3+} ions, magnetic chains of spin-5/2 Fe_3Y clusters had been identified and described. The substitution of the nonmagnetic Y^{3+} ion by the magnetic Gd^{3+} adds magnetic interactions to the clusters, but not magnetic anisotropy. The heat capacity measurement shows an excess over the contribution of the antiferromagnetically coupled Fe_3Gd magnetic clusters at very low temperature, which can be described as magnetic spin-1 chains using a Blume–Capel model. The intercluster interaction constant $\mathcal{J}_{ch} = -55(5)$ mK is very similar to that of $\{Fe_3YO_2\}$, which shows that the interaction is mainly controlled by the magnitude of the cluster's magnetic moment.

Keywords: single molecule magnets, molecular magnetism, 1D magnetism, single chains magnets.

1. Introduction

Some polynuclear molecular clusters show single-molecule magnet (SMM) behavior; i.e. they display remanence after the application of a magnetic field while not interacting with their neighboring clusters [1]. When spin slow relaxation behavior dominates, these molecules can be regarded as candidates for spintronic elements [2], in quantum information processing [3–6] or in magnetic cooling [7]. In particular cases, the crystal structure and the intercluster interactions lead to one-dimensional (1D) structures of coupled paramagnetic ions or clusters with magnetic properties similar to those of SMM, which are usually termed single-chain magnets (SCM) [8–10].

Of special interest are bimetallic clusters constituted by transition metals M that provide an important part of the cluster magnetization, and rare earth metals Ln that generate an enhanced magnetic anisotropy by intracluster interactions [11, 12]. In this class of $\{M_xLn_y\}$ clusters, the molecules $[Fe_3Ln(\mu_3\text{–}O)_2(CCl_3COO)_8(H_2O)(THF)_3]$, in brief $\{Fe_3LnO_2\}$, comprise a series of isostructural compounds that allow comparison of their magnetic properties as a function of the different Ln substitutions [13]. All members of this series have a "butterfly" type $\{Fe_3Ln(\mu_3\text{–}O)_2\}^{8+}$ core. The three Fe^{3+} ions form a triangle (Fig. 1), Fe_3, with the Fe2 atom at the body of the butterfly and the two Fe1 and Fe3 atoms at the wings. All Fe^{3+} ions are in the $S = 5/2$ high spin state and the Fe1–Fe2 exchange interaction is antiferromagnetic ($\mathcal{J}/k_B = -50$ K), while that of Fe1–Fe3 is negligible, yielding to a total spin $S_T = 5/2$ for the Fe_3 subcluster [14]. The Fe_3–Ln intracluster interaction within the "butterfly" molecule (for magnetic Ln lanthanide) is also antiferromagnetic [14]. The intensity of the intracluster interaction was evaluated in a combined study of conventional magnetometry and X-ray magnetic circular dichroism as a function of an applied magnetic field, both in the case of Kramers ions as Ln = Gd and Dy [15] and non-Kramers ions as Ln = Tb and Ho [16, 17].

The reference case where Ln is substituted by a non-magnetic ion, $\{Fe_3YO_2\}$, has been recently studied at very low temperature (16 mK < T < 20 K), especially with regard

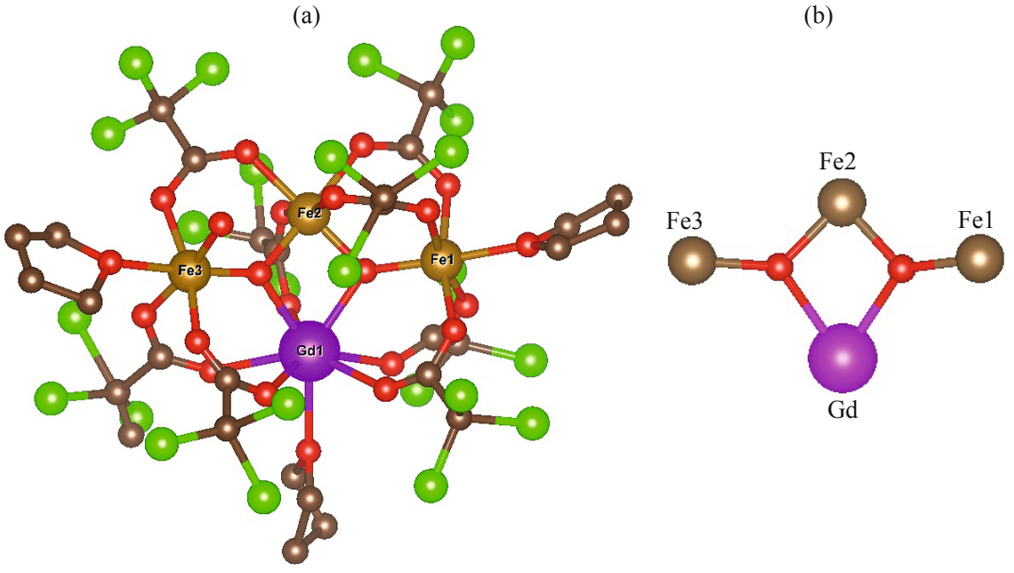

Fig. 1. (Color online) (a) The molecule $[Fe_3Ln(\mu_3\text{–}O)_2(CCl_3COO)_8(H_2O)(THF)_3]$ (water molecule and hydrogen atoms not included). (b) The Fe_3Gd cluster with the bonding oxygen ions.

to its magnetic relaxation behavior [18]. Its heat capacity and static magnetic susceptibility showed uniaxial anisotropy of the Fe^{3+} ions, which could be treated as a Fe_3 cluster with anisotropy ($D/k_B = -0.56(3)$ K), and an unexpected, very weak additional antiferromagnetic intercluster interaction along a zigzag chain ($\mathcal{J}_{ch}/k_B = -40(2)$ mK). When no external magnetic field is applied ($H = 0$) the magnetic relaxation is very fast and can be explained as caused by quantum tunneling of the magnetization through the anisotropy barrier, while for $H = 6.5$ kOe two relaxation processes are induced, a slow direct process, affected by phonon bottleneck effects, and a fast one due to the single chain magnet behavior with activation energy $E_a/k_B = 3.4(6)$ K, arising from single-molecule magnetic anisotropy and spin-spin correlations along the chains.

The goal of this work is to determine the effect of Ln substitution on the magnetic chains using Gd, of null or negligible anisotropy. We will show that the magnetic chains are also present in the $\{Fe_3GdO_2\}$ butterfly, and propose possible structures of those chains.

2. Experimental details

The synthesis of the $[Fe_3Ln(\mu_3\text{–}O)_2(CCl_3COO)_8(H_2O)(THF)_3]$ compounds is briefly reviewed in Refs. 13, 19. The $\{Fe_3GdO_2\}$ samples were in powder form. Heat capacity $C(T)$ under different applied magnetic fields (0–80 kOe) was measured on powder samples embedded in vacuum grease to enhance thermal contact using a Quantum Design PPMS. Experiments in the low-temperature region ($0.35\ \text{K} < T < 10$ K) were carried out with a ^{3}He refrigerator, while for temperatures ranging between 2 and 20 K the base PPMS system was used. The coincident temperature range ($2\ \text{K} < T < 10$ K) was intended to overlap the low T to the absolute high T measurements. Measurements under zero magnetic field were carried out up to 100 K.

3. Results and discussion

The case of the $\{Fe_3GdO_2\}$ compound is quite different from that of the Y substitution, since both the Fe_3 subcluster and the Gd^{3+} ion contribute to the magnetic heat capacity. The molar specific heat C/R of $\{Fe_3GdO_2\}$ measured as a function of temperature is shown in Fig. 2(a). The lattice contribution may dominate the heat capacity above 5 K, but unlike the $\{Fe_3YO_2\}$ compound, there is no clear temperature range where a BT^n dependence ($n \approx 3$) can be used unambiguously to subtract this non-magnetic contribution. Since at above about 10 K the specific heat of the Gd and Y compounds are very similar, both compounds are isostructural, their lattice parameters differ by less than 1% and their molecular masses by 3.4%, we will use as an estimate for the lattice contribution that of the Y compound [18], i.e., $B/R = 8.42(8)\cdot10^{-3}\ \text{K}^{-3}$.

The $\{Fe_3LnO_2\}$ butterfly molecule consists of a magnetic Fe_3 subcluster coupled to the magnetic moment of the Ln^{3+} ion. The substitution by the non-magnetic Y^{3+} ion allowed us to study the magnetic properties of the Fe_3 subclusters and their interactions. The Hamiltonian for the subcluster, $\mathcal{H}_0^{Fe3}$, is the multi-spin Hamiltonian in the Heisenberg–Dirac–van Vleck approximation of isotropic exchange interaction, which may include ligand field anisotropy

$$\mathcal{H}_0^{Fe3} = -2\mathcal{J}\left(\mathbf{S}_1^{Fe}\cdot\mathbf{S}_2^{Fe} + \mathbf{S}_2^{Fe}\cdot\mathbf{S}_3^{Fe}\right) - 2\mathcal{J}'\left(\mathbf{S}_1^{Fe}\cdot\mathbf{S}_3^{Fe}\right) + \mathcal{H}_{LF}^{(Fe3)}, \quad (1)$$

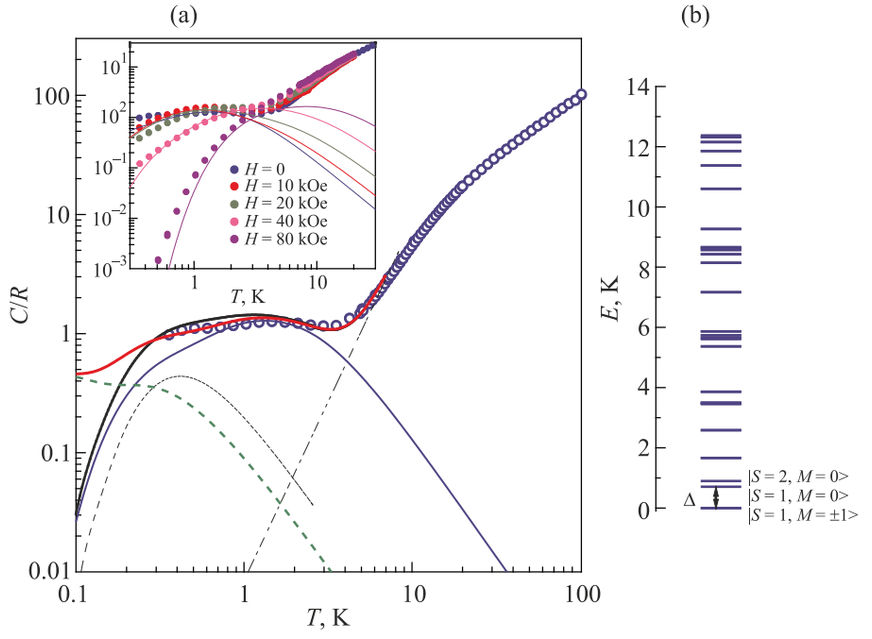

Fig. 2. (Color online) (a) Experimental heat capacity and magnetic contributions to the heat capacity: Fe_3Gd dimer exchange interaction and Fe_3 cluster anisotropy (——), chains of Fe_3Gd clusters as Ising (– –) and Blume–Capel models (– –), lattice contribution (·– ·–) and the addition of all contributions for $\mathcal{J}^{Fe3Gd}/k_B = -0.25$ K, $D^{Fe3}/k_B = -0.56$ K, $\mathcal{J}_{ch}/k_B = -0.055$ K using the Ising (——) and Blume–Capel (——) models. Inset: Heat capacity under an external applied field. Full lines: Calculated heat capacity with and without the chain's contribution. (b) Single dimer cluster energy level scheme; $|S,M\rangle$ represent the dimer states.

with spin operators $\mathbf{S}_1^{Fe}$, $\mathbf{S}_2^{Fe}$, $\mathbf{S}_3^{Fe}$, and $S_i^{Fe} = 5/2$, acting on the $\mathbf{S}_1^{Fe} \otimes \mathbf{S}_2^{Fe} \otimes \mathbf{S}_3^{Fe}$ wave function complete base of dimension 216. As shown earlier [6, 20], given the strong antiferromagnetic Fe–Fe intracluster interaction in $\mathcal{H}_0^{Fe3}$ within the Fe_3 subcluster $\mathcal{J} = -50$ K and $\mathcal{J}' \approx 0$ up to temperatures ~ 200 K the Fe_3 electronic state may be represented by a total subcluster spin $S^{Fe3} = 5/2$, with sixfold degenerate wave functions $|S^{Fe3} = 5/2, S_z^{Fe3}\rangle$ split in three doublets by an effective magnetic uniaxial anisotropy of ligand field interaction origin, which for $\{Fe_3YO_2\}$ is described by the perturbative LF Hamiltonian acting on the total S^{Fe3} subcluster eigenfunction base

$$\mathcal{H}_{LF}^{(Fe3)} = D^{Fe3}\left[\left(S_z^{Fe3}\right)^2 - \frac{1}{3}S^{Fe3}\left(S^{Fe3}+1\right)\right]. \qquad (2)$$

The Hamiltonian of Eq. (2) in itself could not account for an excess of specific heat below ~ 1 K. The associated entropy of this excess pointed to additional degrees of freedom, which was interpreted as intercluster interactions of the Fe_3 subclusters forming magnetic chains. This could be described within a 1D Ising model of $S = 5/2$ spins with uniaxial anisotropy. Thus, the Hamiltonian including the Fe_3–Fe_3 interaction $\mathcal{J}_{ch}^{Fe3}$ is

$$\mathcal{H}_{ch}^{(Fe3)} = -2\mathcal{J}_{ch}^{Fe3}\sum_{i=1}^{N} S_z^{Fe3}(i)S_z^{Fe3}(i+1) + D^{Fe3}\sum_{i=1}^{N}\left(S_z^{Fe3}\right)^2(i). \qquad (3)$$

The very low-temperature heat capacity and dc magnetic susceptibility of $\{Fe_3YO_2\}$ were successfully described with this model, with the parameters $D^{Fe3}/k_B = -0.56$ K and $J_{ch}^{Fe3}/k_B = -40$ mK.

When a magnetic Ln^{3+} ion is present in the $\{Fe_3LnO_2\}$ butterfly, the magnetic properties of the Fe_3Ln cluster can be described at low temperature through the Hamiltonian

$$\mathcal{H}^{cluster} = \mathcal{H}_0^{(Fe3)} + \mathcal{H}^{Ln} + \mathcal{H}^{Ln-Fe3} + \mathcal{H}_Z, \qquad (4)$$

where $\mathcal{H}_0^{(Fe3)}$ corresponds to the Fe_3 subcluster Hamiltonian Eq. (1), projected on the subcluster total spin states $|S^{Fe3} = 5/2, S_z^{Fe3}\rangle$. $\mathcal{H}^{Ln}$ corresponds to the ligand field splitting of the ground multiplet of the Ln^{3+} ion. In the case of Ln = Gd^{3+}, whose intrinsic magnetic anisotropy is expected to be negligible, this term will not be considered.

The Gd–Fe_3 interaction is described by a Heisenberg–Dirac–van Vleck Hamiltonian

$$\mathcal{H}^{Gd-Fe3} = -2\sum_{\alpha=x,y,z}\mathcal{J}_\alpha^{Fe3Gd} J_\alpha S_\alpha^{Fe3}, \qquad (5)$$

where $\mathcal{J}_\alpha$ are the diagonal terms of the anisotropic exchange tensor, and J is the angular moment of the ground state multiplet of Gd^{3+} ($J = 7/2$). For lanthanides with magnetic anisotropy, J can be substituted by an effective spin S^* for temperatures lower than the first excited level.

Finally, if an external magnetic field **H** is applied, a Zeeman term is present

$$\mathcal{H}_Z = \left(\hat{g}^{\mathrm{Fe3}}\mu_B \mathbf{S}^{\mathrm{Fe3}} + \hat{g}^{\mathrm{Gd}}\mu_B \mathbf{J}\right)\cdot \mathbf{H} \qquad (6)$$

with $\hat{g}^{\mathrm{Gd}}$ the g tensor for Gd.

These Hamiltonian operators act on the dimer wave functions $\phi(S^{\mathrm{dim}}, S_z^{\mathrm{dim}}) = |\, S^{\mathrm{Fe3}} J S^{\mathrm{dim}} S_z^{\mathrm{dim}}\rangle$ constructed as the linear combination with Clebsch–Gordon coefficients, of the product wave functions of the Fe_3 subcluster spin $|\, S^{\mathrm{Fe3}} = 5/2, S_z^{\mathrm{Fe3}}\rangle$ and the Ln single ion wave functions $|\, J = 7/2, J_z\rangle$.

As a first approximation, the specific heat can be calculated using: (i) the exchange interaction in the Fe_3–Gd dimer with $J = 7/2$, $S^{\mathrm{Fe3}} = 5/2$, $H = 0$, and $g = 2$, i.e., considering that there is no magneto-crystalline anisotropy in the Gd^{3+} ion, and described by the Hamiltonian Eq. (4) with isotropic exchange $\mathcal{J}^{\mathrm{Fe3Gd}}/k_B = -0.25$ K as proposed from a previous $M(H)$ measurement at 1.8 K [3], and (ii) the anisotropy is expected to come only from the Fe_3 cluster ($D^{\mathrm{Fe3}}/k_B = -0.56$ K) [18]. The calculated constant volume heat capacity (PHI code was used [20]) C_V, with the lattice contribution added, is shown in Fig. 2. The cluster's energy levels are shown in Fig. 2(b), where we note that the ground state is a $S^{\mathrm{dim}} = 1$ triplet, split into a ground doublet with $S_z^{\mathrm{dim}} = \pm 1$, and an excited singlet, with $S_z^{\mathrm{dim}} = 0 =$ at $\Delta = 0.71$ K. These lowest energy dimer wave functions are predominantly composed of the $J = 7/2$ and $S^{\mathrm{Fe3}} = 5/2$ antiferromagnetically coupled spins.

In Fig. 2 (Inset) the specific heat under external magnetic fields up to $H = 80$ kOe is also shown, along with the calculations with the same interaction parameters set as used with the zero field specific heat. The case of $H = 0$ is also included in the Inset for comparison.

Below ≈ 0.8 K, there is an excess of the experimental heat capacity, as it had been observed in the $\{Fe_3YO_2\}$ butterfly, where it was explained as originated from chains of S^{Fe3} spins of the Fe_3 subclusters [20]. Down to the lowest temperature of the present measurements of the heat capacity (0.35 K), there is no indication of a close magnetic transition at a lower temperature, and the maximum excess in C is $\approx 0.34R$ at 0.35 K, below the Ising value of $0.42R$. A contribution to the heat capacity of that value at very low temperature from hyperfine interactions can be discarded since for Gd^{3+} it is the lowest of the lanthanide series by at least an order of magnitude [21].

The specific heat of the Ising chain is readily calculated as

$$C_V/R = \left[\frac{2\mathcal{J}_{\mathrm{ch}}\sigma^2}{k_B T}\,\mathrm{sech}\left(\frac{2\mathcal{J}_{\mathrm{ch}}\sigma^2}{k_B T}\right)\right]^2 \qquad (7)$$

with $\sigma = \pm S$. The interaction constant along spin-5/2 chains in $\{Fe_3YO_2\}$, $\mathcal{J}_{\mathrm{ch}} = -0.040$ K, can be scaled to spin-1 as $\mathcal{J}_{\mathrm{ch}} = -0.25$ K. The chains contribution from Eq. 7 is added to that of the $\{Fe_3Gd\}$ cluster and is shown in Fig. 2. The agreement is apparently good, in view of the approximations used, particularly the transfer of the unmodified Fe_3 subcluster zero field splitting parameter D^{Fe3} [Eq. (2)] and chain interaction constant $\mathcal{J}_{\mathrm{ch}}$ obtained for $\{Fe_3YO_2\}$ to $\{Fe_3GdO_2\}$, which shows that the anisotropy at the Gd^{3+} sites is actually negligible, even at very low temperature in this compound, and it does not affect the interactions within and between the clusters.

However, unlike the case of $\{Fe_3YO_2\}$, the use of the Ising chain in $\{Fe_3GdO_2\}$ suffers from some inconsistency because the Ising model only takes into account the ground state doublet. While in $\{Fe_3YO_2\}$ the two lowest doublets ($S_z^{\mathrm{Fe3}} = \pm 5/2$ and $\pm 3/2$) are separated by an energy interval $|\,4D^{\mathrm{Fe3}}/k_B\,| = 2.24$ K, the first excited energy level in $\{Fe_3GdO_2\}$ (a singlet) is only 0.71 K above the ground state doublet [Fig. 2(b)], and thus it should be well populated at temperatures between 0.35 and 0.8 K. Indeed since the intercluster interaction should be of dipolar origin, and it is modeled approximately as 1D magnetic system of chains with much smaller interchain interactions, the change from spins 5/2 in $\{Fe_3YO_2\}$ to spins 1 in $\{Fe_3GdO_2\}$ should entail much lower interaction energy between next neighboring angular moments, $2\mathcal{J}_{\mathrm{ch}}(S^{\mathrm{dim}})^2$. It is also worth noting that the intercluster distances in the Y and Gd compounds are very similar, thus the difference in intercluster interaction energy would be mainly due to the cluster angular moment magnitude.

The levels scheme of Fig. 2 shows that more states should be taken into account. The first excited state is a singlet at $\Delta/k_B = 0.71$ K, whose main $|\, S^{\mathrm{Fe3}}, S_z^{\mathrm{Fe3}}\rangle$ and $|\, J, J_z\rangle$ components yield a dimer state $\approx |\, S^{\mathrm{dim}} = 1, S_z^{\mathrm{dim}} = 0\rangle$. Above, the next level lies at ≈ 0.9 K from the ground state energy, but its single ion components give a dimer singlet state $\approx |\, S^{\mathrm{dim}} = 2, S_z^{\mathrm{dim}} = 0\rangle$, of non collinear coupling of angular moments. Then, instead of the Ising model, we will use a Blume–Capel model [22] with spin $S = S^{\mathrm{dim}} = 1$ triplet and effective anisotropy $D^{\mathrm{eff}} = -\Delta/2$. The calculation of the specific heat in this model was performed using the transfer matrix method [23–25]. The calculated specific heat with this added contribution is displayed in Fig. 2 for $\mathcal{J}_{\mathrm{ch}}/k_B = -0.055(5)$ K. The very good agreement with the experimental results demonstrates that the intercluster magnetic interactions already shown in $\{Fe_3YO_2\}$ are also present in the Gd compound, and the value of the interaction constant, very similar to that of the $\{Fe_3YO_2\}$, is consistent with an interaction mainly controlled by the magnetic moments of the clusters in these two isostructural compounds with close cell parameters.

The structure of the magnetic chains in the crystal structure of $\{Fe_3GdO_2\}$ should be related to the expected dipolar interaction type between the Fe_3Gd magnetic clusters. However, there is yet no evidence or calculations on the direction of the anisotropy axes of the Fe^{3+} ions and that of the effective anisotropy of the Fe_3Gd cluster, determined exclusively by the Fe^{3+} ions. The structure of both $\{Fe_3YO_2\}$ and $\{Fe_3GdO_2\}$ shows the $P2_1$ space group and two formula units *per* unit cell, i.e., two butterfly molecules related by

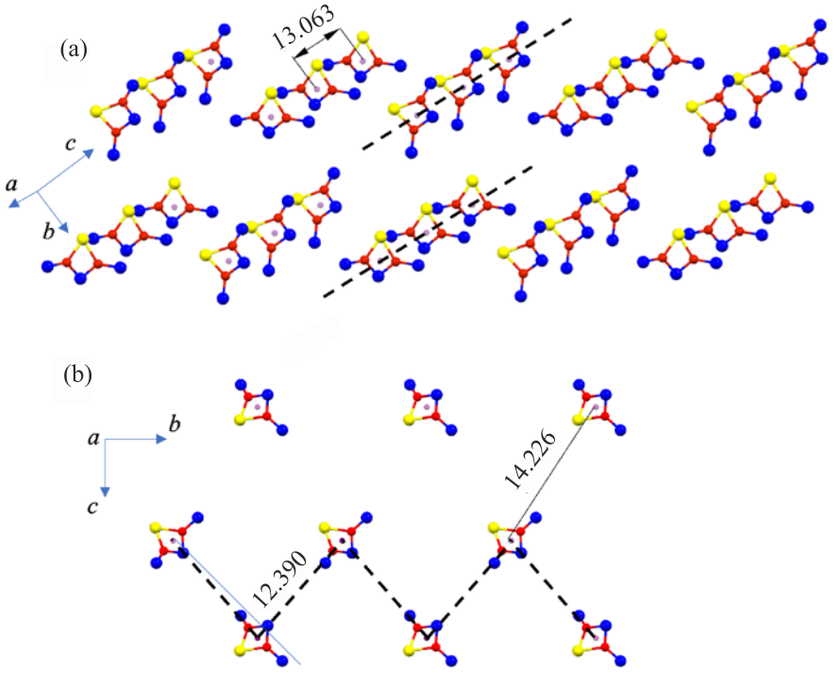

Fig. 3. (Color online) (a) The network of Fe_3Gd clusters showing the straight chains (dashed lines) formed from clusters along the crystallographic *a* axis. (b) The network is viewed along the *a* axis. The dashed lines show the previously proposed chain of the closest Fe_3Gd clusters. In the figure, the upper row of clusters is not on the same plane as the middle and lower row. Color code: Fe^{3+} (blue), Gd^{3+} (yellow), μ_3–O (red), centroids (brown). Distances are given in Å.

the 2_1 screw rotation, which makes the mean planes of these two Fe_3 clusters perpendicular to each other. Previously, for the Y case, [18] a zigzag chain of these two molecules related by the 2_1 symmetry was suggested, where the distance between neighboring centroids of Fe_3 clusters is the shortest possible centroids distance. In order to have parallel angular moments in that chain's structure, the anisotropy axis was suggested to lie close to a direction onto the Fe_3 mean plane. An alternative chain's structure can also be proposed, which places fewer restrictions on the anisotropy axes to have the Ising-like chains (Fig. 3). In the $\{Fe_3GdO_2\}$ compound the second shortest distance between centroids of the Fe_3Gd clusters is 13.063 Å, corresponding to the crystallographic *a* axis, and in this chain all molecules display the same orientation and are located in a straight line, since all are related by a lattice translation. Therefore, all clusters in a chain will share the same magnetic anisotropy axis, and consequently, the angular moments should be parallel or antiparallel irrespective of the direction of the anisotropy axis. Adjacent parallel chains of the same type include Fe_3Gd centroids separated by the shortest intercluster distance (12.390 Å), but their relative orientations are linked by the 2_1 screw axis, thus the directions of angular moments on adjacent chain will not be parallel unless the anisotropy axis at each cluster is parallel or normal to that symmetry axis.

4. Conclusions

The $[Fe_3Ln(\mu_3\text{–}O)_2(CCl_3COO)_8(H_2O)(THF)_3]$ complexes, with Ln = Y and Gd, show intracluster and intercluster magnetic interactions of the $\{Fe_3YO_2\}$ and $\{Fe_3GdO_2\}$ "butterfly" shaped units. The intercluster interactions are reflected as an excess of entropy over the intracluster contribution, shown through very low-temperature heat capacity measurements. As in the previously reported $\{Fe_3YO_2\}$, the intercluster interactions can be modeled as magnetic chains. In the Gd "butterfly", the magnetic Gd^{3+} ion couples antiferromagnetically to the Fe_3 subcluster, producing an energy spectrum of close levels, but it does not introduce magnetic anisotropy. However, the magnetic chains persist as if formed by magnetic clusters of spin 1. When this 1D magnetic system is analyzed in the framework of a Blume–Capel model, the obtained interaction constant is very similar to that of $\{Fe_3YO_2\}$, which may be associated with the dipolar nature of the intercluster interactions.

In the present report, an alternative spatial structure of the chains to that presented for $\{Fe_3YO_2\}$ is introduced, which is simpler and allows for more flexibility for directions of the coupled magnetic moments. The absence of anisotropy in Gd^{3+} leaves the Fe_3 subcluster as the sole source of magnetic anisotropy, which may explain the persistence of magnetic chains $\{Fe_3GdO_2\}$ in spite of the substitution of the nonmagnetic Y^{3+} ions by the magnetic Gd^{3+} one.

The series of isostructural $\{Fe_3LnO_2\}$ magnetic molecular system includes Ln = Dy, Ho, and Tb, all of them highly anisotropic, whose uniaxial anisotropy axis will force directions for the $\{Fe_3Ln\}$ clusters, which could prevent the formation of magnetic chains, while for the isotropic Ln = Y and Gd that direction is determined by the anisotropy of the Fe_3 subclusters. A study to address this hypothesis is underway.

Acknowledgments

We acknowledge financial support from the Spanish Agencia Estatal de Investigaciyn, through projects PID2020-115159GB-I00/AEI/10.13039/501100011033, Aragonese project RASMIA E12_20R co-funded by Fondo Social Europeo and the European Union FEDER (ES). The authors would like to acknowledge the use of the Servicio General de Apoyo a la Investigaciyn-SAI, Universidad de Zaragoza.

1. D. Shao and X. Wang, *Chin. J. Chem.* **38**, 1005 (2020).
2. E. Burzuri and H. van der Zaant, *Molecular magnets: Physics and applications*, Springer, Berlin (2014), Chap. *Single Molecule Spintronics*, p. 297.
3. M. N. Leuenberger and D. Loss, *Nature* **410**, 789 (2001).
4. M. Affronte and F. Troiani, *Potentialities of molecular nanomagnets for information technology*, Springer, Berlin (2014), Chap. *Single Molecule Spintronics*, p. 249.
5. K. V. Hoogdalem, D. Stepanenko, and D. Loos, *Molecular magnets for quantum information processing*, Springer, Berlin (2014), Chap. *Single Molecule Spintronics*, p. 275.
6. M. Mannini, F. Pineider, C. Danieli, F. Totti, L. Sorace, P. Sainctavit, M. Arrio, E. Otero, L. Joly, J. C. Cezar, A. Cornia, and R. Sessoli, *Nature* **468**, 417 (2010).
7. M. Evangelisti, *Molecule-based magnetic coolers: Measurement, design and application*, Springer, Berlin (2014), Chap. *Single Molecule Spintronics*, p. 365.
8. H.-L. Sun, Z.-M. Wang, and S. Gao, *Coord. Chem. Rev.* **254**, 1081 (2010).
9. D. Gatteschi and A. Vindigni, *Molecular magnets: Physics and applications*, Springer, Berlin (2014), Chap. *Single Chain Magnets*, p. 297.
10. C. Coulon, V. Pianet, M. Urdampilleta, and R. Clérac, *Molecular nanomagnets and related phenomena*, Springer-Verlag, Berlin, Heidelberg (2015), Chap. *Single-Chain Magnets and Related Phenomena*, p. 143.
11. J. Luzón and R. Sessoli, *Dalton Trans.* **41**, 13556 (2012).
12. J. Tang, I. Hewitt, N. T. Madhu, G. Chastanet, W. Wernsdorfer, C. E. Anson, C. Benelli, R. Sessoli, and A. K. Powell, *Angew. Chemie -Int. Ed.* **45**, 1729 (2006).
13. V. Mereacre, D. Prodius, C. Turta, S. Shova, G. Filoti, J. Bartolomé, R. Clérac, C. E. Anson, and A. K. Powell, *Polyhedron* **28**, 3017 (2009).
14. J. Bartolomé, G. Filoti, V. Kuncser, G. Schinteie, V. Mereacre, C. E. Ansona, A. K. Powell, D. Prodius, and C. Turta, *Phys. Rev. B* **80**, 014430 (2009).
15. L. Badía-Romano, F. Bartolomé, J. Bartolomé, J. Luzón, D. Prodius, C. Turta, V. Mereacre, F. Wilhelm, and A. Rogalev, *Phys. Rev. B* **87**, 184403 (2013).
16. L. Badía-Romano, J. Rubín, F. Bartolomé, J. Bartolomé, J. Luzón, D. Prodius, C. Turta, V. Mereacre, F. Wilhelm, and A. Rogalev, *Phys. Rev. B* **92**, 064411 (2015).
17. L. Badía-Romano, J. Rubín, F. Bartolomé, J. Bartolomé, J. Luzón, D. Prodius, C. Turta, V. Mereacrea, F. Wilhelm, and A. Rogalev, *J. Magn. Magn. Mater*. **400**, 137 (2016).
18. J. Rubín, L. Badía-Romano, F. Luis, V. Mereacre, D. Prodius, A. Arauzo, F. Bartolomé, and J. Bartolomé, *Dalton Trans.* **49**, 2979 (2020).
19. C. Turta, D. Prodius, V. Mereacrea, S. Shova, M. Gdaniec, Y. Simonov, V. Kuncser, G. Filoti, A. Caneschi, and L. Sorace, *Inorg. Chem. Commun.* **7**, 576 (2004).
20. N. F. Chilton, R. P. Anderson, L. D. Turner, A. Soncini, and K. S. Murray, *J. Comput. Chem.* **34**, 1164 (2013).
21. B. Abragam and B. Bleaney, *Electron Paramagnetic Resonance of Transition Ions*, Oxford University Press, Oxford (1970), Chap. 5.
22. H. W. Capel, *Physyca* **32**, 966 (1966).
23. M. Lines, *Phys. Rev. Lett.* **42**, 533 (1979).
24. I. Chatterjee, *J. Math. Phys*. **25**, 2339 (1984).
25. I. Chatterjee, *Phys. Rev. B* **34**, 7969 (1986).

Низькотемпературні магнітні взаємодії у сполуці типу «метелик» $\{Fe_3GdO_2\}$: стійкість магнітних ланцюжків

J. Rubín, A. Arauzo, F. Bartolomé, D. Prodius, J. Bartolomé

Наведено вимірювання теплоємності у випадку Ln = Gd серії молекул «метеликів» $[Fe_3Ln(\mu_3\text{–}O)_2(CCl_3COO)_8(H_2O)(THF)_3]$, скорочено $\{Fe_3LnO_2\}$. У раніше вивченій сполуці типу «метелик» $\{Fe_3YO_2\}$, де магнітні властивості походять лише від іонів Fe^{3+}, магнітні ланцюжки спін-5/2 кластерів Fe_3Y були ідентифіковані та описані. Заміна немагнітного іона Y^{3+} на магнітний Gd^{3+} додає кластерам магнітну взаємодію, але не магнітну анізотропію. Вимірювання теплоємності показує перевищення над внеском антиферомагнітно пов'язаних магнітних кластерів Fe_3Gd за дуже низьких температур, які можна описати як магнітні спін-1 ланцюжки за допомогою моделі Блюма–Капеля. Константа міжкластерної взаємодії $J_{ch} = -55{,}5(5)$ мК дуже схожа на константу $\{Fe_3YO_2\}$, яка показує, що взаємодія переважно контролюється величиною магнітного моменту кластера.

Ключові слова: одномолекулярні магніти, молекулярний магнетизм, 1D магнетизм, одноланцюжкові магніти.